Title

An ANGPTL4—ceramide—protein kinase Cζ axis mediates chronic glucocorticoid exposure—induced hepatic steatosis and hypertriglyceridemia in mice

Journal

Journal of Biological Chemistry, 294(23)

ISSN

0021-9258

Authors

Chen, Tzu-Chieh

Lee, Rebecca A

Tsai, Sam L

et al.

Publication Date

2019-06-01

DOI

10.1074/jbc.ra118.006259

An ANGPTL4–ceramide–protein kinase Cζ axis mediates chronic glucocorticoid exposure–induced hepatic steatosis and hypertriglyceridemia in mice

Received for publication, October 13, 2018, and in revised form, May 1, 2019 Published, Papers in Press, May 3, 2019, DOI 10.1074/jbc.RA118.006259

Tzu-Chieh Chen[‡§1], Rebecca A. Lee[‡¶1], Sam L. Tsai[‡], Deepthi Kanamaluru[‡], Nora E. Gray[‡§], Nicholas Yiv[‡], Rachel T. Cheang[‡], Jenna H. Tan[‡], Justin Y. Lee[‡], Mark D. Fitch[‡], Marc K. Hellerstein[‡], and Jen-Chywan Wang[‡§¶2]

From the [‡]Department of Nutritional Sciences & Toxicology, the [§]Metabolic Biology Graduate Program, and the [¶]Endocrinology Graduate Program, University of California–Berkeley, Berkeley, California 94720-3104

Edited by George M. Carman

Chronic or excess glucocorticoid exposure causes lipid disorders such as hypertriglyceridemia and hepatic steatosis. Angptl4 (angiopoietin-like 4), a primary target gene of the glucocorticoid receptor in hepatocytes and adipocytes, is required for hypertriglyceridemia and hepatic steatosis induced by the synthetic glucocorticoid dexamethasone. Angptl4 has also been shown to be required for dexamethasone-induced hepatic ceramide production. Here, we further examined the role of ceramide-mediated signaling in hepatic dyslipidemia caused by chronic glucocorticoid exposure. Using a stable isotope-labeling technique, we found that dexamethasone treatment induced the rate of hepatic *de novo* lipogenesis and triglyceride synthesis. These dexamethasone responses were compromised in Angptl4-null mice (Angptl4$^{-/-}$). Treating mice with myriocin, an inhibitor of the rate-controlling enzyme of *de novo* ceramide synthesis, serine palmitoyltransferase long-chain base subunit 1 (SPTLC1)/SPTLC2, decreased dexamethasone-induced plasma and liver triglyceride levels in WT but not Angptl4$^{-/-}$ mice. We noted similar results in mice infected with adeno-associated virus– expressing small hairpin RNAs targeting Sptlc2. Protein phosphatase 2 phosphatase activator (PP2A) and protein kinase Cζ (PKCζ) are two known downstream effectors of ceramides. We found here that mice treated with an inhibitor of PKCζ, 2-acetyl-1,3-cyclopentanedione (ACPD), had lower levels of dexamethasone-induced triglyceride accumulation in plasma and liver. However, small hairpin RNA–mediated targeting of the catalytic PP2A subunit (Ppp2ca) had no effect on dexamethasone responses on plasma and liver triglyceride levels. Overall, our results indicate that chronic dexamethasone treatment induces an ANGPTL4–ceramide–PKCζ axis that activates hepatic *de novo* lipogenesis and triglyceride synthesis, resulting in lipid disorders.

Chronic exposure to glucocorticoids has long been associated with the development of lipid disorders including dyslipidemia and hepatic steatosis (1–3). In contrast, reducing glucocorticoid levels, such as inhibiting 11β-hydroxysteroid dehydrogenase type 1, an enzyme converting inactive glucocorticoids to active hormones, reduces plasma and liver TG levels in animal models of metabolic syndrome (4–7) and nonalcoholic fatty liver disease patients (8). In fact, an inhibitor for 11β-hydroxysteroid dehydrogenase type 1 is currently under clinical trial phase 1b, which showed a modest but significant improvement of nonalcoholic fatty liver disease (NAFLD)[3] (8). Antagonists for the glucocorticoid receptor (GR) also improve plasma lipid profiles (9, 10). Despite these long-established observations, the mechanisms governing these glucocorticoid effects are not entirely clear. Chronic glucocorticoid exposure has been shown to induce *de novo* lipogenesis (DNL) and triglyceride (TG) synthesis in liver (11, 12). However, treating hepatocytes with glucocorticoids alone does not always promote lipogenesis (13, 14). Thus, the induction of hepatic DNL and TG synthesis by chronic glucocorticoid exposure may require additional signals or the effects of glucocorticoids on other tissues.

It has been proposed that the excess lipolysis induced by GC in white adipose tissue plays a role in the development of dyslipidemia and fatty liver (15, 16). This proposed mechanism is in agreement with previous observations showing that glucocorticoid-induced hepatic steatosis and hypertriglyceridemia are dependent on the presence of *Angptl4* (*angiopoietin-like 4*), a GR primary target gene (17). *Angptl4* encodes a secreted protein that can promote intracellular lipolysis in adipocytes (18). It has been shown that glucocorticoid-stimulated lipolysis in white adipose tissue is attenuated in mice lacking *Angptl4* (*Angptl4*$^{-/-}$) and purified ANGPTL4 protein directly induces lipolysis in mouse primary adipocytes (18). Thus, it is conceivable that Angptl4 mediates glucocorticoid stimulation of lipolysis in white adipose tissue, which mobilizes fatty acids to the liver for TG synthesis and storage. Notably, Angptl4 has also been shown to be required for glucocorticoids to stimulate hepatic ceramide production, which activates protein phosphatase 2A and protein kinase Cζ (PKCζ) to suppress insulin signaling in liver (19). Because hepatic ceramide levels have been posi-

This work is supported by National Institutes of Health Grants R01DK083591 and R01DK113019 (to J. C. W.). The authors declare that they have no conflicts of interest with the contents of this article. The content is solely the responsibility of the authors and does not necessarily represent the official views of the National Institutes of Health.

This article contains Table S1.

[1] These authors contributed equally to this work.

[2] To whom correspondence should be addressed: 315 Morgan Hall, University of California Berkeley, Berkeley, CA 94720-3104. E-mail: walwang@berkeley.edu.

[3] The abbreviations used are: NAFLD, nonalcoholic fatty liver disease; shRNA, small hairpin RNA; ACPD, 2-acetyl-1,3-cyclopentanedione; PKC, protein kinase C; GR, glucocorticoid receptor; DNL, *de novo* lipogenesis; TG, triglyceride; Dex, dexamethasone; PPAR, peroxisome proliferator-activated receptor; qPCR, quantitative PCR; AAV, adeno-associated virus.

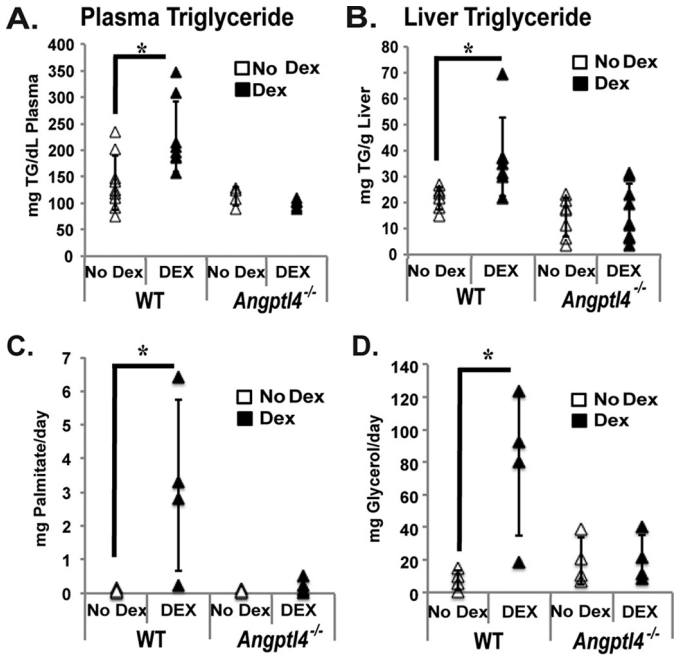

Figure 1. Angptl4 is required for chronic dexamethasone treatment-activated DNL and TG synthesis. WT and *Angptl4*$^{-/-}$ mice were treated with or without dexamethasone (2.5 mg/kg body weight) in drinking water for 7 days. At day 6, the mice were given a priming intraperitoneal bolus injection of 99.9% labeled with heavy water (^2H_2O) that contains 0.9% (w/v) sodium chloride to quickly raise the concentration of heavy water in body water to ~5%. This 5% ^2H_2O concentration was maintained by *ad libitum* administration of 8% ^2H_2O drinking water throughout the 24-h labeling period. *A* and *B*, at the end of treatment, the levels of TG in plasma (*A*) and liver (*B*) were measured. The *error bars* represent standard deviation ($n = 5–7$). *, $p < 0.05$. Moreover, the fatty acids and glycerol-moieties of TGs isolated from liver were analyzed by GC-MS to quantify the mass isotopomer abundances. *C* and *D*, the absolute rate of DNL (*C*) and TG synthesis (*D*) were calculated based on ^2H incorporation into TG-palmitate and TG-glycerol and their respective measured pool sizes in the tissue. The *error bars* represent standard deviation ($n = 4$). *, $p < 0.05$.

tively associated with NAFLD (20–22), we hypothesize that glucocorticoid-induced Angptl4-dependent hepatic production or ceramides are involved in the development of hepatic steatosis and hypertriglyceridemia. In this study, we examined this model and also identified the downstream effectors of ceramide-mediated signaling that mediate glucocorticoid response on hepatic TG homeostasis.

Results

Chronic dexamethasone exposure–induced hepatic DNL and TG synthesis was attenuated in Angptl4$^{-/-}$ *mice*

Male WT and *Angptl4*$^{-/-}$ mice were treated with or without dexamethasone (a synthetic glucocorticoid) for 7 days. At the end of the treatment, blood and liver were collected, and plasma and liver TG levels were measured. Dexamethasone treatment significantly elevated plasma and liver TG levels in WT mice (Fig. 1, *A* and *B*). These dexamethasone effects were suppressed in *Angptl4*$^{-/-}$ mice (Fig. 1, *A* and *B*). To examine whether dexamethasone treatment stimulates hepatic DNL and TG synthesis and the role of Angptl4 in these processes, we applied a stable isotope labeling technique. In the liver of PBS-treated WT mice, the absolute rate of DNL (mg palmitate synthesized over a 24-h labeling period) was 0.08 mg palmitate/day/mouse (Fig. 1*C*). Dexamethasone treatment for 7 days resulted in a 40-fold induction in the absolute DNL rate (3.2 mg palmitate/day; Fig. 1*C*). In contrast, the absolute rate of DNL in the liver of untreated *Angptl4*$^{-/-}$ mice was 0.09 mg palmitate/day (Fig. 1*C*). Dexamethasone treatment increased the rate of DNL 2.4-fold (to 0.22 mg palmitate/day; Fig. 1*C*). This induction was markedly lower than the dexamethasone response in liver of WT mice ($p < 0.05$). These results demonstrate that Angptl4 is involved chronic dexamethasone exposure–stimulated hepatic DNL.

Dexamethasone treatment also resulted in 6-fold induction of the absolute rate of TG synthesis in the liver of WT mice (Fig. 1*D*). The absolute TG synthesis rate in liver of untreated *Angptl4*$^{-/-}$ mice was not statistically significantly different from untreated WT mice (Fig. 1*D*). Dex treatment did not elevate the absolute hepatic TG synthesis rate in *Angptl4*$^{-/-}$ mice (Fig. 1*D*). These results demonstrate that without Angptl4, the ability of Dex to augment TG synthesis in the liver was diminished.

The ability of dexamethasone to induce lipogenic genes in liver was attenuated without Angptl4

We analyzed the expression of genes involved in DNL and TG synthesis in the liver of WT and *Angptl4*$^{-/-}$ mice treated with or without dexamethasone. We found that the expression of genes encoding enzymes in DNL and TG synthesis, such as *Fasn*, *Acaca*, *Acacb*, *Dgat2*, *Gpat1*, and *Lpin1*, were increased by dexamethasone in WT mice liver (Fig. 2*A*). In *Angptl4*$^{-/-}$ mice, the ability of Dex to activate these genes was significantly reduced (Fig. 2*A*). Interestingly, dexamethasone treatment significantly reduced the expression of *Srebp1c*, a transcription factor that activates the transcription of many lipogenic genes (23, 24), in WT mice liver (Fig. 2*A*). In *Angptl4*$^{-/-}$ mice, the reduction of *Srebp1c* expression by dexamethasone was even more profound (Fig. 2*A*). In contrast, the expression of *Chrebpβ*, another transcription factor that augments lipogenic gene transcription (25), was markedly enhanced in WT but not *Angptl4*$^{-/-}$ mice liver (Fig. 2*A*). The expression of *Chrebpα*, a longer isoform of *Chrebp* (24, 26), however, was not affected by dexamethasone (Fig. 2*A*). However, the expression of *Chrebpα* was still reduced in *Angptl4*$^{-/-}$ mice liver (Fig. 2*A*). The fact that *Srebp1c* expression was reduced by chronic dexamethasone exposure raised a question regarding whether Srebp1c was activated to promote lipogenic and TG synthetic gene transcription. Interestingly, protein levels of the mature and the immature forms of Srebp1c in the whole cell extracts and the mature form of Srebp1c in the nuclear extracts isolated from control and dexamethasone-treated liver were similar (Fig. 2*B*). These results demonstrated that despite the reduction of *Srebp1c* mRNA by dexamethasone treatment, Srebp1c protein levels were not significantly decreased by dexamethasone treatment for the time period conducted in our experiments. We performed ChIP experiments to further examine the recruitment of Srebp1c to its binding site in the *Fasn* gene. We found that Srebp1c was recruited to the *Fasn* gene promoter without dexamethasone treatment, which likely provides the basal lipogenic action (Fig. 2*C*). Dexamethasone treatment further enhanced the Srebp1c recruitment to the *Fasn* gene promoter (Fig. 2*C*). These results are in agreement with the increased lipogenic rate in the livers of dexamethasone-treated mice.

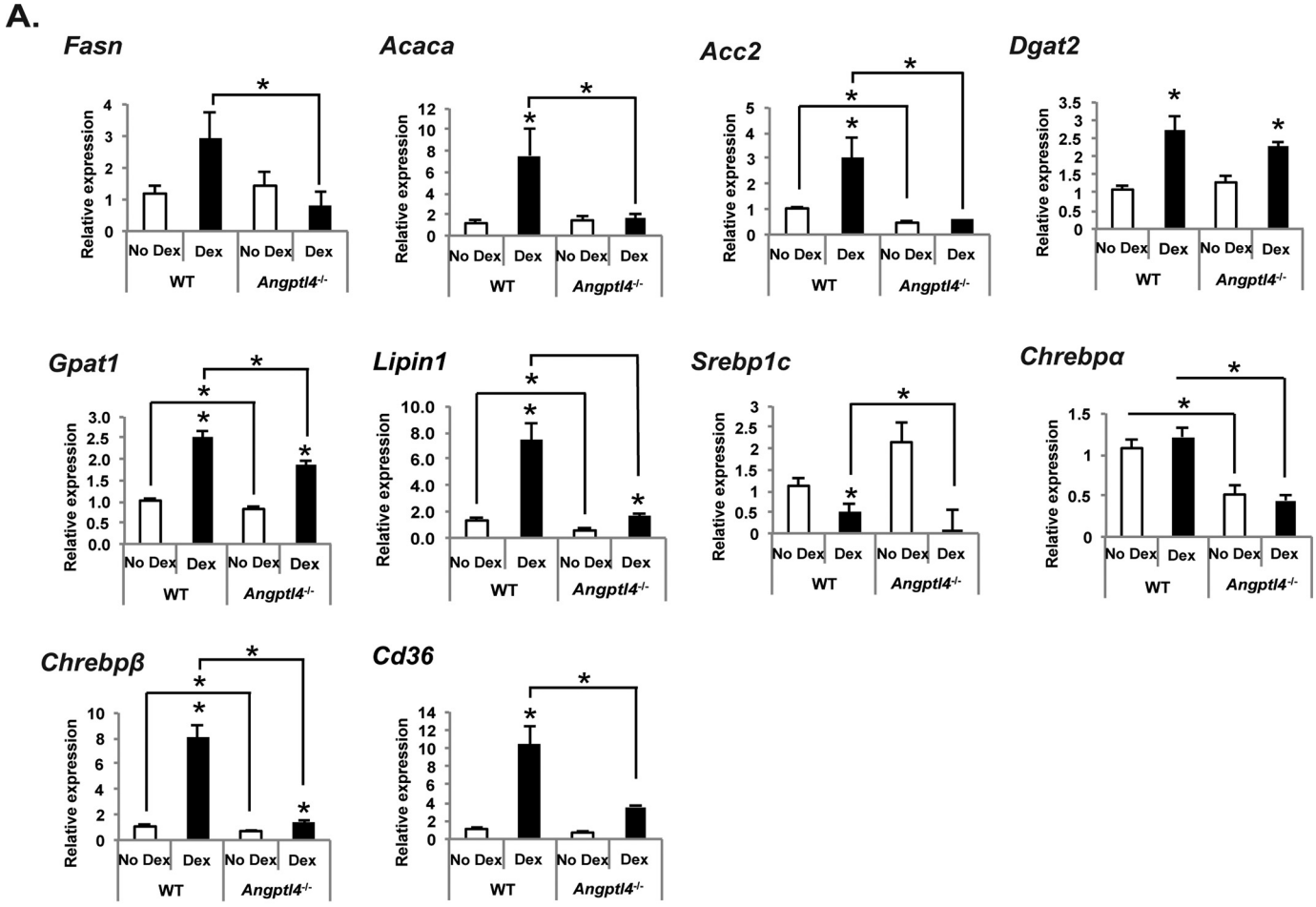
A.
Fasn
Acaca
Acc2
Dgat2
Gpat1
Lipin1
Srebp1c
Chrebpα
Chrebpβ
Cd36
Relative expression
No Dex
Dex
WT
Angptl4-/-

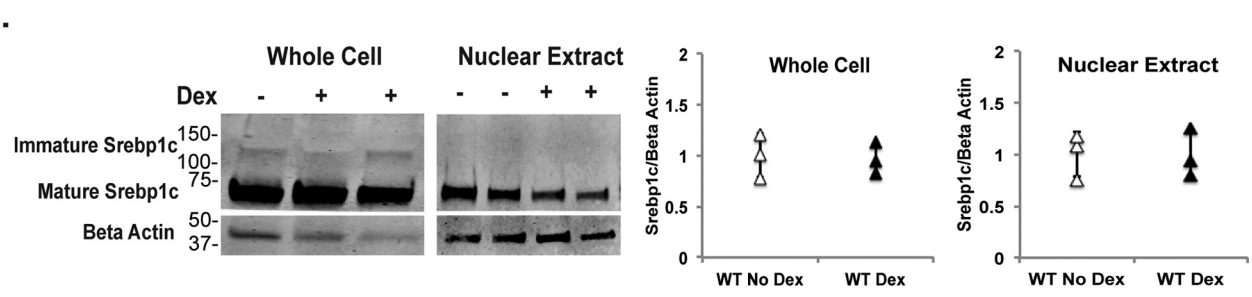
B.
Whole Cell
Nuclear Extract
Dex
Immature Srebp1c
Mature Srebp1c
Beta Actin
150-
100-
75-
50-
37-
Srebp1c/Beta Actin
WT No Dex
WT Dex

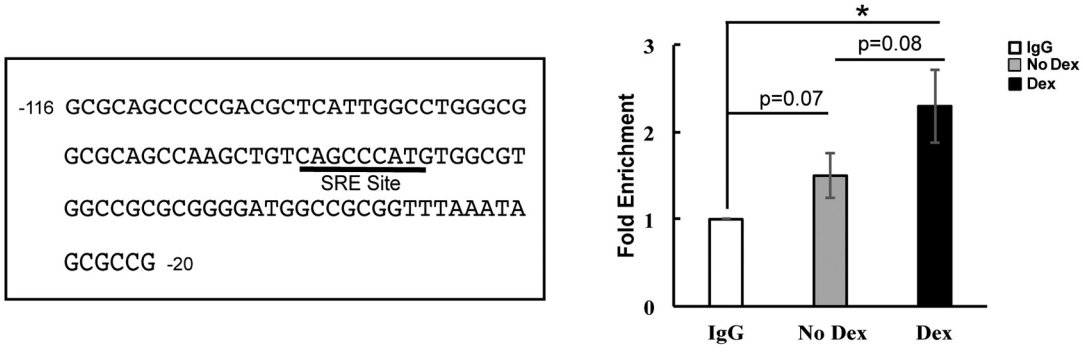
C.
-116 GCGCAGCCCCGACGCTCATTGGCCTGGGCG
GCGCAGCCAAGCTGTCAGCCCATGTGGCGT
SRE Site
GGCCGCGCGGGGATGGCCGCGGTTTAAATA
GCGCCG -20
Fold Enrichment
p=0.07
p=0.08
IgG
No Dex
Dex

A ceramide synthesis inhibitor reduced chronic dexamethasone exposure–increased plasma and liver TG levels

We previously showed that chronic dexamethasone exposure increased the accumulation of various species of ceramides in the liver of WT mice, and these dexamethasone effects were attenuated in the liver of *Angptl4*$^{-/-}$ mice (19). To examine whether ceramides are involved in dexamethasone-induced hepatic steatosis and hypertriglyceridemia, WT and *Angptl4*$^{-/-}$ mice were treated with dexamethasone, and with or without myriocin, an inhibitor of serine palmitoyltransferase 1 and 2 (Spt1/2), rate-controlling enzymes in the *de novo* ceramide synthesis pathway (27). Dexamethasone treatment was for 7 days, whereas myriocin was included in the final 4 days. Myriocin treatment decreased TG levels in both the plasma and the liver of dexamethasone-treated WT mice (Fig. 3, *A* and *B*). The TG levels in liver of dexamethasone-treated *Angptl4*$^{-/-}$ mice were significantly lower than those of dexamethasone-treated WT mice (Fig. 3, *A* and *B*). However, in dexamethasone-treated *Angptl4*$^{-/-}$ mice, myriocin did not further reduce the TG levels in plasma and liver (Fig. 3, *A* and *B*). These results suggest that increased ceramide production plays a key role in Angptl4 function in dexamethasone-induced TG accumulation in the plasma and the liver.

We next monitored the effect of myriocin on the expression of lipogenic and TG synthetic genes in the liver of myriocin-treated WT and *Angptl4*$^{-/-}$ mice. We found that the expression of lipogenic genes, such as *Fasn*, *Acaca*, and *Chrebpα*, was reduced in the liver of myriocin-treated WT mice (Fig. 3*C*). The expression of *Srebp1c*, *Cd36*, and *Chrebpβ*, although not statistically significant, was also trending lower in myriocin-treated WT mice (Fig. 3*C*). Myriocin treatment did not affect the expression of these genes in *Angptl4*$^{-/-}$ mice. These results suggest that ceramide production is required for Angptl4's role in the induction of lipogenic gene expression by chronic dexamethasone exposure. Interestingly, the expression of TG synthetic genes, such as *Dgat2*, *Gpat1*, and *Lpin1,* was not affected by myriocin treatment. We also found that myriocin increased the expression of *Angptl4* in the liver but not epididymal white adipose tissue of WT mice treated with dexamethasone (Fig. 3*D*).

To further confirm that the hepatic ceramide synthetic pathway is involved in triglyceride accumulation in the plasma and liver, we infected WT mice with adeno-associated virus (serotype 8) expressing scramble (control) small hairpin RNA (shRNA) or shRNA targeting *Sptlc2*, which encodes a rate-controlling enzyme of *de novo* ceramide synthesis. These mice were called AAV8-*shSCR* and AAV8-*shSptlc2*, respectively. We found that hepatic *Sptlc2* expression was significantly lower in the liver of AAV8-*shSptlc2* mice (Fig. 3*E*). Moreover, upon dexamethasone treatment, plasma and liver triglyceride levels were also significantly lower in AAV8-*shSptlc2* mice than those of AAV8-*shSCR* mice (Fig. 3, *F* and *G*. These results are similar to those of the myriocin treatment experiments above (Fig. 3, *A* and *B*).

PKCζ but not PP2A is required for chronic dexamethasone exposure–induced plasma and liver TG accumulation

PKCζ and PP2A are two known downstream effectors of ceramides. To examine whether PP2A is involved in glucose intolerance induced by glucocorticoids, WT mice were infected with adenovirus expressing scrambled shRNA or shRNA targeting *Ppp2ca*, which encodes the PP2A catalytic subunit. These mice were called Ad-*shSCR* and Ad-*shPpp2ca*, respectively. Western blots validated a significant reduction in the protein abundance of Ppp2ca by shRNA in mouse liver (Fig. 4*A*). However, we did not observe significant differences in plasma and liver TG levels between dexamethasone-treated Ad-*shSCR* and Ad-*shPpp2ca* mice (Fig. 4, *B* and *C*).

To test the role of PKCζ in glucocorticoid-induced hepatic hypertriglyceridemia, WT and *Angptl4*$^{-/-}$ mice were injected with or without 2-acetyl-1,3-cyclopentanedione (ACPD), an inhibitor of atypical PKC, PKCζ, and PKCι (28, 29) for the final 4 days of the 7-day dexamethasone course. Western blots showed that ACPD treatment reduced the levels of phosphorylated PKCζ in liver (Fig. 5*A*), which indicates reduced PKCζ activity. We found that ACPD treatment reduced both plasma and liver TG accumulation in WT but not *Angptl4*$^{-/-}$ mice (Fig. 5, *B* and *C*). Based on these results, PKCζ but not PP2A is involved in chronic dexamethasone-induced hepatic steatosis and hypertriglyceridemia.

To confirm whether PKCζ is downstream of ceramides, we performed Western blots to monitor phosphorylated PKCζ levels in the liver of dexamethasone-treated WT and *Angptl4*$^{-/-}$ mice that were treated with or without myriocin. We found that the relative ratio of phosphorylated PKCζ and total phosphorylated PKCζ was reduced in liver of WT mice (Fig. 5*D*). These results confirmed that ceramide production is involved in chronic dexamethasone treatment-induced PKCζ activity. We also found that *Angptl4* expression was decreased by ACPD treatment in epididymal white adipose tissue but not liver of WT mice (Fig. 5*E*).

The antagonist of PPARα did not affect chronic dexamethasone exposure–induced plasma and liver TG accumulation

PPARα has been previously implicated in the production of ceramides in various cell types (30–32). Moreover, PPARα has been shown to be involved in glucocorticoid-induced hepatic gluconeogenesis and insulin resistance (33). We therefore examine whether PPARα is involved in dexamethasone treatment–induced plasma and liver triglyceride accumulation.

Figure 2. Chronic dexamethasone treatment-induced expression of genes involved in hepatic TG homeostasis was reduced in *Angptl4*$^{-/-}$ mice. *A*, WT and *Angptl4*$^{-/-}$ mice were treated with or without dexamethasone (0.84 mg/kg body weight) in drinking water for 7 days. RNA from the liver of these mice was isolated, and real-time PCR was performed to monitor the expression of genes involved in hepatic TG homeostasis. The *error bars* represent S.E. ($n = 7–8$). *, $p < 0.05$. *B*, whole cell and nuclear extracts were prepared from WT and *Angptl4*$^{-/-}$ mice treated with and without dexamethasone for 7 days. Extracts were proved for Srebp1c levels that were normalized to β-actin. The *error bars* represent standard deviation ($n = 3$). *, $p < 0.05$. *C*, mouse *Fasn* promoter sequences between −116 and −20 relative to the transcription start site were amplified by ChIP primers. SRE site is labeled (49). Srebp1c ChIP was performed in the liver of WT mice treated with or without dexamethasone (0.84 mg/kg body weight) in drinking water for 7 days. The *error bars* represent S.E. ($n = 5$). *, $p < 0.05$.

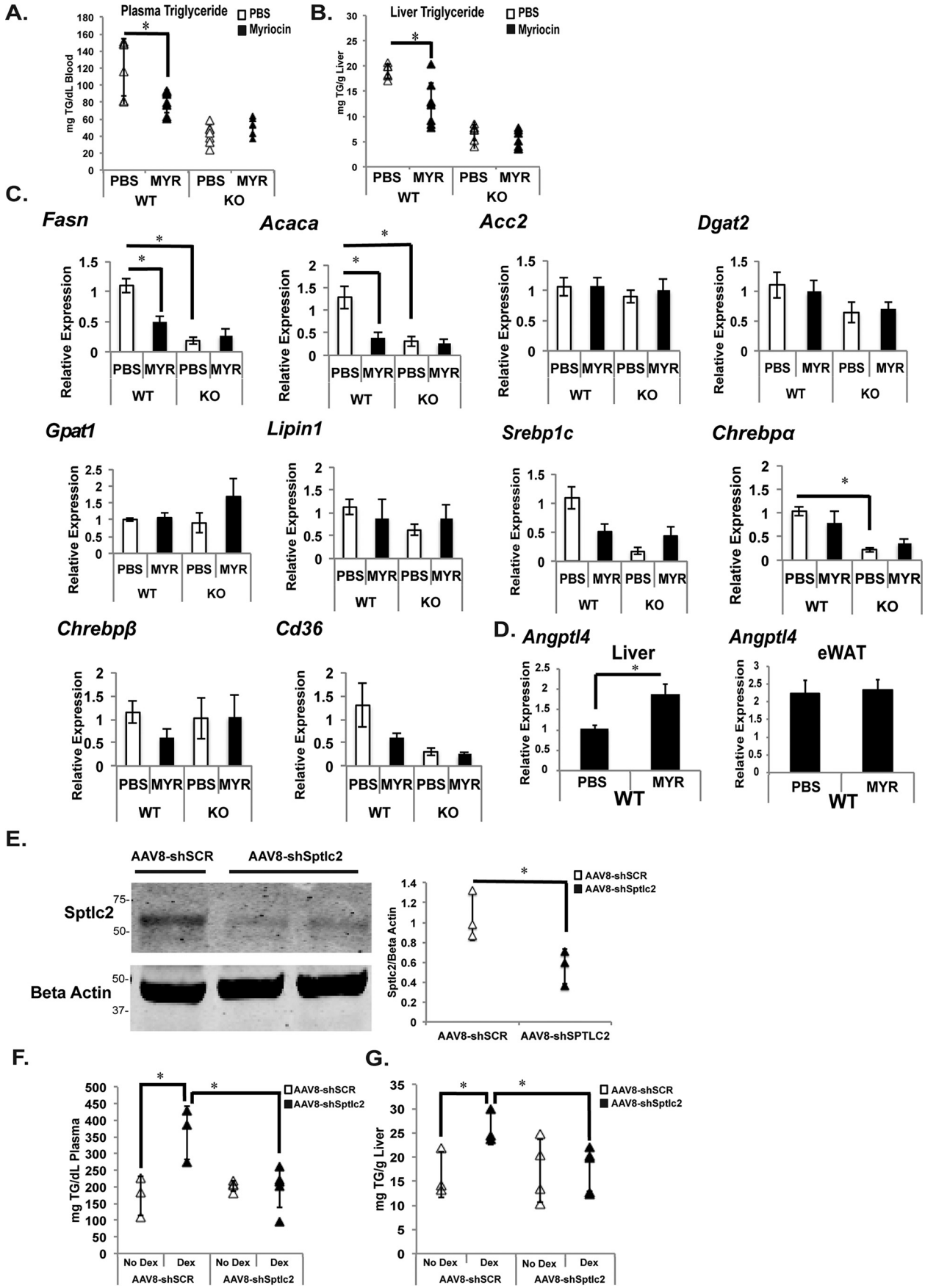
A.
Plasma Triglyceride
PBS
Myriocin
mg TG/dL Blood
PBS MYR PBS MYR
WT KO
B.
Liver Triglyceride
PBS
Myriocin
mg TG/g Liver
PBS MYR PBS MYR
WT KO
C.
Fasn
Acaca
Acc2
Dgat2
Gpat1
Lipin1
Srebp1c
Chrebpα
Chrebpβ
Cd36
Relative Expression
PBS MYR PBS MYR
WT KO
D.
Angptl4
Liver
Angptl4
eWAT
Relative Expression
PBS MYR
WT
E.
AAV8-shSCR
AAV8-shSptlc2
Sptlc2
Beta Actin
75-
50-
50-
37-
Sptlc2/Beta Actin
AAV8-shSCR
AAV8-shSPTLC2
F.
mg TG/dL Plasma
AAV8-shSCR
AAV8-shSptlc2
No Dex Dex No Dex Dex
AAV8-shSCR AAV8-shSptlc2
G.
mg TG/g Liver
AAV8-shSCR
AAV8-shSptlc2
No Dex Dex No Dex Dex
AAV8-shSCR AAV8-shSptlc2

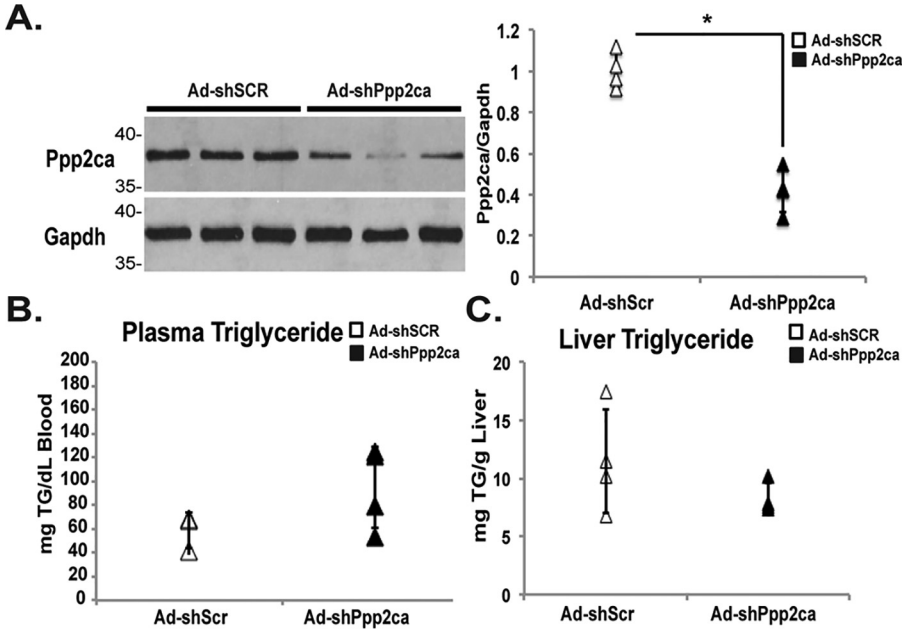

Figure 4. Reducing the expression of Ppp2ca did not affect chronic dexamethasone exposure–induced hepatic steatosis and hypertriglyceridemia. WT mice were infected with adenovirus expressing scramble shRNA or shRNA targeting Ppp2ca. Two days post-infection, the mice were treated with dexamethasone (0.84 mg/kg body weight) in drinking water for 7 days. *A*, at the end of treatment, liver was isolated, and Western blotting was performed to confirm the reduction of Ppp2ca expression in Ad-*shPpp2ca* mice. *B* and *C*, the intensity of the bands was normalized to Gapdh, and plasma (*B*) and liver (*C*) TG were measured in these mice. The *error bars* represent standard deviation ($n = 4$). *, $p < 0.05$.

WT mice treated with dexamethasone were treated with PBS or a PPARα antagonist GW-6471. GW-6471 treatment improved glucose tolerance in dexamethasone-treated mice (Fig. 6*A*). These results were in agreement with the previous observation that showed the improvement of dexamethasone-regulated glucose homeostasis in *PPARα* knockout mice (33). However, GW-6471 treatment did not affect the accumulation of plasma and liver triglyceride levels in mice under dexamethasone treatment (Fig. 6, *B* and *C*).

Discussion

Dyslipidemia is one of the major adverse effects caused by chronic and/or excess glucocorticoid exposure. However, the mechanisms underlying this alteration are mostly unclear. Here we showed that dexamethasone treatment for 7 days elevated hepatic DNL and TG synthesis. Interestingly, previous studies show that glucocorticoid treatment alone on primary hepatocytes or hepatoma cells usually does not promote lipogenesis and/or TG synthesis (11, 12). This suggests that glucocorticoid effects on cell types other than hepatocytes are required for the enhancement of hepatic DNL and TG synthesis. Here we showed that Angptl4-dependent hepatic ceramide production is involved in chronic dexamethasone treatment-induced hepatic steatosis and hypertriglyceridemia (Fig. 7). *Angptl4* is a GR primary target gene encoding a secreted protein that inhibits lipoprotein lipase through its N-terminal coiled-coil domain (34, 35) and promotes intracellular lipolysis in adipocytes via a C-terminal fibrinogen-like domain (36). Such extrahepatic functions of Angptl4 perfectly fit into the model, in which tissues other than liver are involved in chronic glucocorticoid responses on lipid homeostasis. However, it is unclear which function of Angptl4 mediates the dexamethasone response on hepatic DNL and TG synthesis. We propose that the lipolytic activity of Angptl4 is required for promoting the mobilization of fatty acids from white adipose tissue to the liver for ceramide production because palmitoyl-CoA is a precursor of *de novo* ceramide synthesis. Notably, the role of Angptl4 in glucocorticoid-promoted hepatic ceramide production is not limited to providing substrates for *de novo* ceramide biosynthesis. The induction of genes encoding enzymes in the ceramide synthetic pathway by chronic dexamethasone treatment also requires Angptl4 (19). Nonetheless, we have not excluded the potential involvement of the LPL inhibitory activity of Angptl4 in chronic glucocorticoid exposure–induced lipid disorders. Future studies to explore the metabolic source of hepatic ceramides will be of interest. Animal models that specifically disable either function of Angptl4 are needed to address this question.

Hepatic ceramide levels have been associated with NAFLD. However, the exact mechanisms of how ceramide-initiated

Figure 3. Myriocin (*MYR*) treatment reduced chronic dexamethasone exposure–induced hepatic steatosis and hypertriglyceridemia. WT and *Angptl4*$^{-/-}$ mice were treated with dexamethasone (0.84 mg/kg body weight) in drinking water for 7 days. Half of the mice received daily intraperitoneal injections of myriocin (0.5 mg/kg body weight) on days 4–7. *A* and *B*, at the end of treatment, the levels of TG in plasma (*A*) and liver (*B*) were measured. The *error bars* represent standard deviation ($n = 6–8$). *, $p < 0.5$. *C*, RNA from the liver of these mice was isolated, and the expression of genes involved in TG homeostasis was monitored by real-time PCR. The *error bars* represent S.E. ($n = 7–9$). *, $p < 0.05$. *D*, liver and epididymal white adipose tissue RNA was isolated, and gene expression for *Angptl4* was measured. The *error bars* represent S.E. ($n = 7–9$). *, $p < 0.05$. WT mice were infected with adeno-associated virus (AAV8) expressing shRNA for scramble or Sptlc2 and were treated with dexamethasone for 2 weeks. *E*, liver was harvested and analyzed for decreased expression of *Sptlc2*. *F* and *G*, plasma (*F*) and liver (*G*) triglyceride levels were measured. The *error bars* represent standard deviation ($n = 3–4$). *, $p < 0.05$.

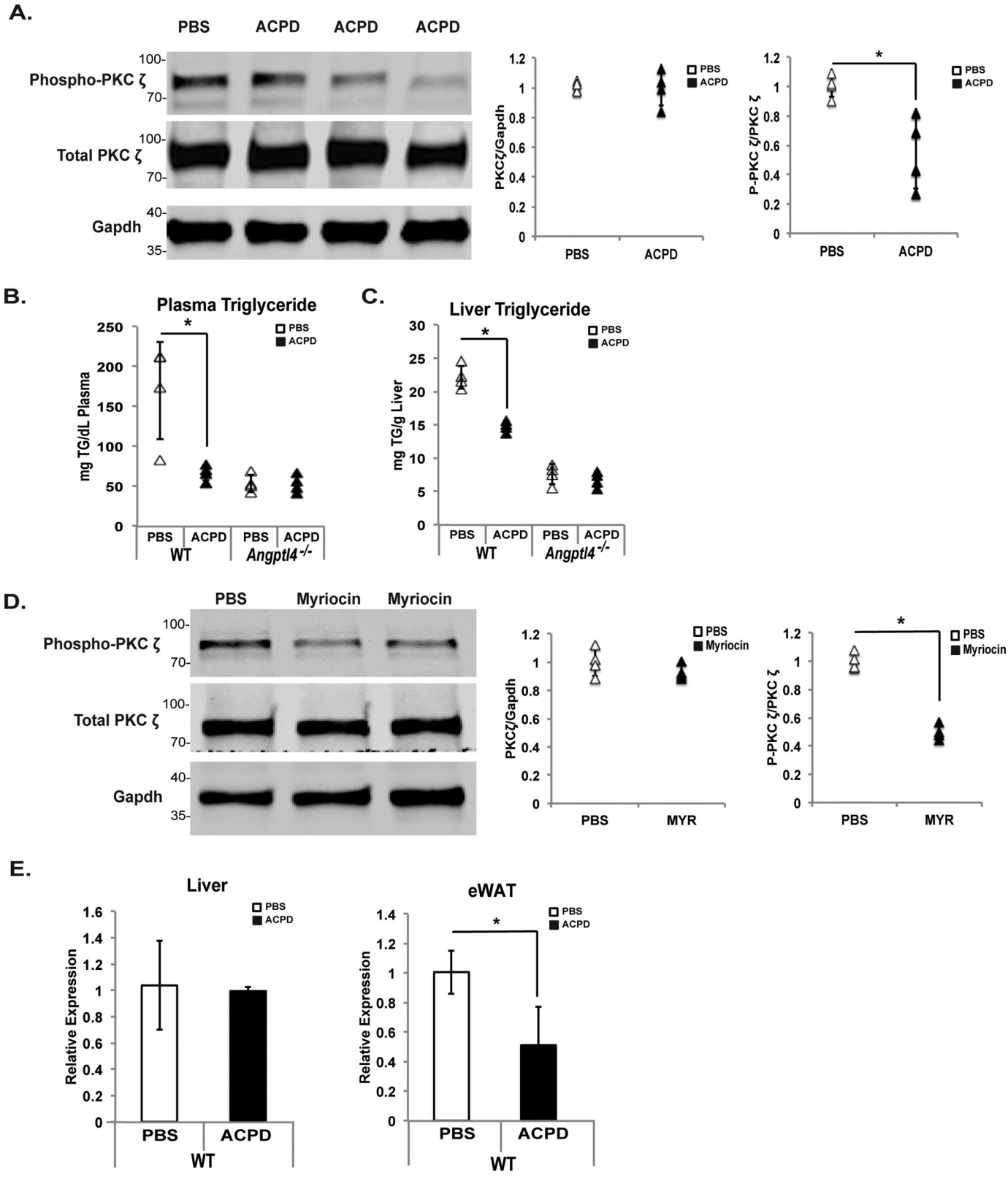

Figure 5. ACPD treatment reduced chronic dexamethasone exposure–induced hepatic steatosis and hypertriglyceridemia. WT and *Angptl4*$^{-/-}$ mice were treated with dexamethasone (0.84 mg/kg body weight) in drinking water for 7 days. Half of the mice of each group were receiving daily subcutaneous injection of ACPD (10 mg/kg body weight, dissolved in PBS) on days 4–7. *A*, at the end of treatment, liver was isolated, and Western blotting was performed to confirm the reduced levels of phosphorylated PKCζ. The intensity of the bands were normalized to Gapdh. The relative ratio of phosphorylated PKCζ to PKCζ represents the PKCζ activity. *B* and *C*, the levels of TG in plasma (*B*) and liver (*C*) were measured from these mice. The *error bars* represent standard deviation ($n = 4$). *, $p < 0.05$. *D*, Western blotting was performed to monitor the levels of phosphorylated PKCζ in the liver of 7-day dexamethasone-treated WT mice that received daily intraperitoneal injection of PBS or myriocin (*MYR*) (0.5 mg/kg body weight) in the final 4 days. *E*, liver and epididymal white adipose tissue RNA were isolated, and gene expression for *Angptl4* was measured. The *error bars* represent standard deviation ($n = 4$). *, $p < 0.05$.

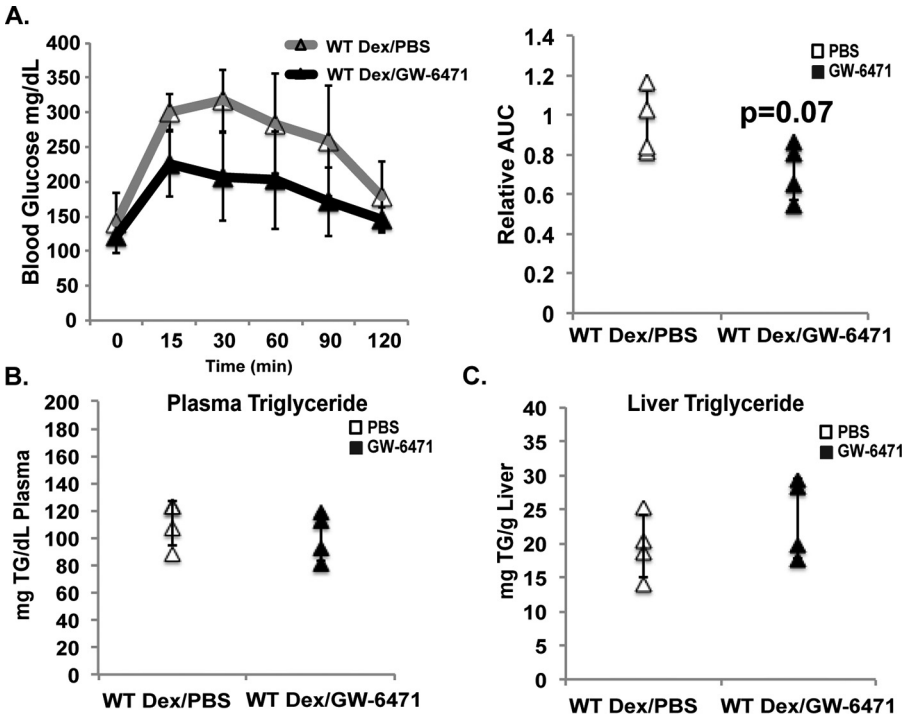

Figure 6. PPARα antagonist GW-6471 may improve glucose tolerance under dexamethasone exposure but has no effect on plasma and liver triglycerides. WT mice were treated with dexamethasone (0.84 mg/kg body weight) in drinking water for 7 days. Half of the mice received daily subcutaneous injection of GW-6471 (10 mg/kg body weight, dissolved in PBS) on days 4–7. *A*, after 7 days of dexamethasone treatment, the mice were fasted 16 h, an intraperitoneal glucose tolerance test was performed, and the relative area under the curve was calculated. *B* and *C*, the mice were allowed to recover for 2 days, and plasma (*B*) and liver (*C*) triglyceride levels were measured. The *error bars* represent standard deviation ($n = 4$). *, $p < 0.05$.

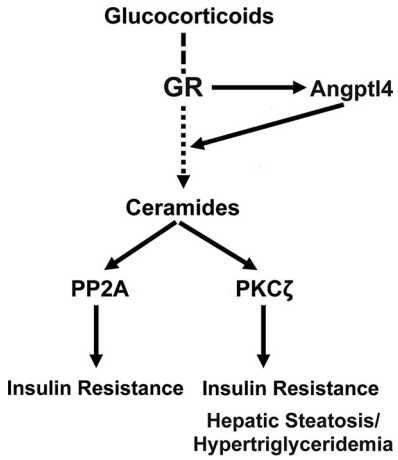

Figure 7. Model of glucocorticoid-induced hepatic steatosis in an *Angptl4*- and ceramide-dependent manner. Glucocorticoids bind to the glucocorticoid receptor, which regulates the expression of primary target genes. *Angptl4* is a glucocorticoid primary target gene that we found to be involved in hepatic ceramide production and hepatic triglyceride accumulation. PP2a and PKCζ are two downstream effectors of ceramides. In our investigation, we found that PKCζ, but not PP2a, was required for glucocorticoid stimulated hepatic triglyceride accumulation.

signaling causes TG accumulation are not entirely clear. Here we found that among two known effectors downstream of ceramides, only PKCζ, but not PP2A, is involved in chronic dexamethasone treatment-induced TG accumulation in liver and plasma (Fig. 6). These results are intriguing because we previously showed that GR-Angptl4-ceramide axis also causes insulin resistance, but that both PKCζ and PP2A were involved in the process (Fig. 7) (19). Insulin resistance has long been associated with the development of dyslipidemia (37–39). The fact that reducing PP2A activity improves insulin sensitivity without affecting plasma and liver TG homeostasis indicates that chronic glucocorticoid exposure–induced lipid disorders are, in certain degrees, independent of insulin resistance. PKCζ has been shown to phosphorylate and mobilize the transcriptional coregulator Baf60c from the cytosol to the nucleus to coactivate with the DNA-binding transcription factor USF1/2 to stimulate transcription of lipogenic genes (40).

Various animal models have been used to study the mechanism of hepatic ceramide-initiated signaling in the regulation of lipid homeostasis. Liver-specific *Cers6* (*ceramide synthase 6*) knockout mice have reduced levels of C16:0 ceramides and are protected from high-fat diet–induced hepatic steatosis (41). In the liver of these mice, fatty acid oxidation is elevated (41). Haploinsufficiency for *Cers2* (*ceramide synthase 2*), which preferentially makes very-long-chain (C22/C24/C24:1) ceramides, led to compensatory increases in C16:0 ceramides and conferred susceptibility to diet-induced steatohepatitis. The inactivation of electron transport chain components in liver of these mice resulted in impaired β-oxidation (42). Moreover, mice overexpressing *Acer2* (*acid ceramidase 2*) in the liver were protected from high-fat diet–induced hepatic steatosis (29). These mice have decreased liver levels of C16:0 and C18:0 ceramides, decreased hepatic fatty acid uptake, and decreased expression of lipogenic genes (29). In agreement with our results, this study also found that PKCζ is involved in ceramide-initiated lipid disorders. Overall, these previous reports indicate that the levels of C16:0 ceramides appear to be associated with excess TG accumulation in liver. Notably, our previous results found that dexamethasone treatment increased the expression of *Cers3*,

Cers4, *Cers5*, and *Cers6* in the liver. Because Cers5 and Cers6 are responsible for the production of C16:0 ceramides, they are two major candidates that mediate dexamethasone response on hepatic lipid metabolism. Future experiments should confirm this model.

Our results also showed that chronic dexamethasone exposure elevated the expression of hepatic lipogenic and TG synthetic genes, which were reduced in *Angptl4*$^{-/-}$ mice. Interestingly, myriocin treatment only reduced the expression of genes involved in DNL but did not affect the dexamethasone response on the expression of TG synthetic genes, such as *Dgat2*, *Lpin1*, and *Gpat1*. This observation is somewhat in agreement with the role of PKCζ in hepatic lipid metabolism. Overexpression of PKCζ in mouse liver strongly increased the expression of lipogenic genes, such as *Fasn*, *Acaca*, and *Srebp1c* (40). *Dgat2* and *Lpin1* were not activated by hepatic PKCζ overexpression, whereas the induction of *Gpat1* was weak (1.3-fold) (40). Based on these results, ceramide-initiated signaling mainly mediates chronic glucocorticoid exposure–induced DNL but not TG synthesis. This notion will need to be further confirmed. Moreover, these gene expression results also suggest that there is another pathway downstream of Angptl4 that regulates *Dgat2* and *Lpin1*.

In conclusion, in this report we identify an Angptl4 – ceramide–PKCζ signaling axis that mediates chronic glucocorticoid exposure–modulated hepatic TG homeostasis. The extensive dissection of this signaling pathway in future studies should identify more novel and specific targets for treating NAFLD and dyslipidemia.

Materials and Methods

Animals

Angptl4$^{-/-}$ mice were provided by the laboratories of Andras Nagy (Samuel Lunenfeld Research Institute, Mount Sinai Hospital) and Jeff Gordon (Washington University) (43). *Angptl4*$^{-/-}$ mice were generated on a mixed B6:129 Sv background. *Angptl4*$^{+/+}$ mice (WT mice) were the littermates of *Angptl4*$^{-/-}$ mice. Male 7–12-week-old mice were used in this study. They were co-housed and were fed a diet of 18% protein, 6% fat (Envigo 2918). The mice were housed in ventilated cages with Sanichip bedding along with a cotton Nestlet and a 4-gm puck of crinkled paper. Genotyping method was performed as previously described (43). Tissues were harvested between 10 and 11 a.m. in the morning, and all plasma triglyceride measurements were performed on unfasted blood. All mice received humane care according the criteria laid out in the Guide for the Care and Use of Laboratory Animals, and the Office of Laboratory Animal Care at the University of California, Berkeley approved all the animal experiments (approval no. AUP-2014-08-6617). The mice were housed on a 12-h light and dark cycle in a temperature-controlled room of ~22 °C.

Stable isotope labeling, mass spectrometric analysis, and calculations

At day 6 of dexamethasone water treatment, the mice were given a priming intraperitoneal bolus injection of 99.9% heavy water (^2H_2O) containing 0.9% (w/v) sodium chloride at 0.035 liter/kg bodyweight to quickly raise the concentration of heavy water in body water to ~5% (Sigma; 151890-250G). This 5% ^2H_2O concentration was maintained for 24 h by *ad libitum* administration of 8% ^2H_2O in the drinking water that was prepared from a 70% deuterium oxide stock (Sigma; 13428-1kg). After 24 h, the mice were sacrificed, and the fatty acids and glycerol moieties of hepatic triglycerides were isolated from the liver. GC-MS was then used to measure the enrichment of mass isotopomers in the TG-fatty acid and TG-glycerol moieties. The fractions of newly synthesized TG-palmitate and TG-glycerol over the 24-h labeling period were calculated by mass isotopomer distribution analysis, with correction for precursor pool ^2H_2O enrichment, as described in detail previously (44, 45).

Drug administration

Male 7–12-week-old *Angptl4*$^{+/+}$ (WT) and *Angptl4*$^{-/-}$ mice were treated with ~2.5 or 0.84 mg/kg of dexamethasone for 7 days through drinking water. Dexamethasone sodium phosphate (Sigma; PHR1768) was dissolved in drinking water (6.5 mg/liter). Dexamethasone sodium phosphate has a molecular weight of 516.4 g/mol, and dexamethasone has a molecular weight of 392.47 g/mol, so there is 760 mg of dexamethasone per gram of dexamethasone sodium phosphate powder. We prepared drinking water that contains 0.00651 g of dexamethasone per liter and based on our estimate that a 30-g mouse drinks ~3.5 ml of water per day. In the myriocin experiments, myriocin (Sigma; M11777-5MG) (0.5 mg/kg body weight) was dissolved in PBS and was injected intraperitoneally to mice on the last 4 days of dexamethasone treatment. For ACPD (Sigma; A155) treatment, the mice were injected subcutaneously with 10 mg/kg of ACPD dissolved in PBS for 4 days. There was no difference in water intake between WT and *Angptl4*$^{-/-}$ mice. In the GW-6471 experiments, GW-6471 (Tocris, Bristol, UK; 4618) (10 mg/kg body weight) (46) was dissolved in 500 μl of DMSO, which was then diluted in PBS to a final concentration of 1 mg/ml and was injected intraperiotoneally on the last 4 days of dexamethasone treatment.

Western blotting

The protein concentration of samples was measured using a BCA protein assay (Thermo Scientific; 23228). Protein (~30 μg) was mixed with 1× NuPAGE LDS sample buffer (Thermo Fisher; NP0007) and 1× NuPAGE sample reducing agent (Thermo Fisher; NP0009) and boiled for 5 min before being applied to SDS-PAGE. The following are the antibodies we used in this study: anti-Gapdh (Santa Cruz Biotechnology; sc-25778), anti–β-actin (Thermo Fisher; MA1140), anti-PKCζ (Santa Cruz Biotechnology; sc-216), anti-phospho-PKCζ (T410; Cell Signaling; 2060S), anti-Ppp2ca (Cell Signaling; 2038S), goat anti-rabbit IRDye 800 (Li-Cor, Lincoln, Nebraska; 926-32211), and anti-Sptlc2 (EMD Millipore, Burlington, MA; ABS1641). The intensity of the bands was quantified using ImageJ software (National Institute of Health) and normalized to Gapdh.

Quantitative real-time PCR

Total RNA was isolated from liver tissues using TRIzol reagent (Invitrogen; 15596018). Reverse transcription was per-

formed as follows: 0.5 μg of total RNA, 4 μl of 2.5 mM dNTP, and 2 μl of 15 μM random primers (New England Biolabs, Ipswich, MA, S1254S) were mixed at a volume of 16 μl and incubated at 70 °C for 5 min. A 4-μl mixture containing 25 units of Moloney murine leukemia virus reverse transcriptase (New England Biolabs; M0253S), 10 units of RNasin Plus (Promega; N261B), and 2 μl of 10× Moloney murine leukemia virus reverse transcriptase reaction buffer (New England Biolabs; B0253S) were added, and samples were incubated at 42 °C for 1 h and then at 95 °C for 5 min. The cDNA was diluted and used for real-time quantitative PCR (qPCR using the Power Eva qPCR SuperMix kit (Biochain, Newark, CA; K5057400), following the manufacturer's protocol. qPCR was performed on the StepOne PCR system (Applied Biosystems) and analyzed with the ΔΔCt method, as supplied by the manufacturer (Applied Biosystems). *Rpl19* gene expression was used for internal normalization. The primer sequences used in this study are listed in Table S1.

Adenovirus and AAV

Adenovirus expressing scramble shRNA or shRNA targeting *Ppp2ca* was purchased from Vector Biolabs (shADV-269223). The targeting sequence for *Ppp2ca* is CGACGAGTGTTTAAGGAAATA, which has been previously reported (47). The mice were injected by tail vein with 1–2 × 10^9 plaque-forming unit adenovirus/mouse. AAV serotype 8 shRNA targeting *Sptlc2* was purchased from Vector Biolabs. The targeting sequence for *Sptlc2* is GCTCATACCAAAGAAATACTT. The mice were injected by tail vein with 4.5 × 10^{11} GC/mouse.

Plasma TG and liver TG measurement

Plasma TG levels were measured using a serum triglyceride determination kit (Sigma; TR0100). Liver was cut into 100-mg pieces, placed in 700 μl of a 3:5 ratio ethanolic KOH and 3 M KOH and 100% EtOH, and incubated overnight at 55 °C. The next day, samples were vortexed well and were spun for 5 min at 5,000 rpm at room temperature. 200 μl of the supernatant was transferred and added to 215 μl of 1 M $MgCl_2$, vortexed, and incubated on ice for 10 min. The samples were then spun for 5 min 5,000 rpm at room temperature, and the supernatant was used to run on a serum triglyceride determination kit (Sigma; TR0100). The concentration of triglyceride was calculated as mg/ml and then was converted to mg triglyceride/g liver by dividing the concentration by 0.069.

Chromatin immunoprecipitation

The protocol for mouse liver ChIP experiment is modified from our previous reported protocol (48). Liver tissues were harvested from male WT mice treated with or without dexamethasone, minced with a razor blade, and collected in 1× SSC buffer (150 mM NaCl and 15 mM sodium citrate). The samples were then washed on a nutator, followed by centrifugation at 4,000 rpm for 3 min at 4 °C to remove supernatant. The liver pellets were resuspended in PBS and cross-linked with 1% formaldehyde for 15 min at room temperature with gentle shaking, and the reaction was quenched with the addition of 125 mM glycine. Centrifugation followed to remove supernatant, and the cell pellets were washed with ice-cold PBS plus protease inhibitor with shaking. Once PBS was removed, the cells were resuspended in hypotonic buffer (10 mM HEPES at pH 7.9, 1.5 mM $MgCl_2$, 10 mM KCl, 0.2% Nonidet P-40, 1 mM EDTA, 5% sucrose) with protease inhibitor, 1.5 mM spermine, and 0.5 mM spermidine added right before use. The cells were homogenized using a Dounce homogenizer for eight strokes each sample. Homogenized cells in hypotonic buffer were mounted onto cushion buffer (10 mM Tris-HCl at pH 7.5, 15 mM NaCl, 60 mM KCl, 1 mM EDTA, 10% sucrose, with protease inhibitor, 1.5 mM spermine, and 0.5 mM spermidine added right before use) and centrifuged at 4,000 rpm at 4 °C for 5 min, followed by the removal of supernatant. SDS sonication buffer (50 mM Tris-HCl at pH 8.0, 2 mM EDTA, and 1% SDS added right before use) was applied to resuspend the nuclei pellet for sonication at 60% output for five cycles, 10 s each. To remove insoluble components, the samples were centrifuged at 13,000 rpm for 15 min at 4 °C, and the supernatant was collected. Then 1 volume of dilution buffer (20 mM Tris-HCl at pH 8.0, 2 mM EDTA, 200 mM NaCl, 1% Triton X-100, and 0.1% sodium deoxycholate) was added to the supernatant and was divided accordingly for immunoprecipitation overnight (4 μg of antibodies: IgG from Santa Cruz Biotechnology (sc-47778), GeneScript (A01008), and Srebp1c from Santa Cruz Biotechnology (sc-1351)). The next day, 30 μl of 50% protein A/G plus-agarose bead slurry was applied, and the samples were nutated for 2 h at 4 °C. The following 500-μl washes were done, all supplemented with protease inhibitor: once with TSE I (20 mM Tris-HCl at pH 8.0, 2 mM EDTA, 150 mM NaCl, 1% Triton X-100, and 0.1% SDS); once with TSE II (20 mM Tris-HCl at pH 8.0, 2 mM EDTA, 500 mM NaCl, 1% Triton X-100, and 0.1% SDS); once with TSE III (10 mM Tris-HCl at pH 8.0, 1 mM EDTA, 0.25 M LiCl, 1% Nonidet P-40, and 1% sodium deoxycholate), and twice with TE buffer (10 mM Tris-HCl at pH 8.0 and 1 mM EDTA). Centrifugation at 8,000 rpm at 4 °C for 1 min was used to remove supernatant between washes. 400 μl of freshly prepared elution buffer (100 mM $NaHCO_3$ and 1% SDS) was added to each sample, and elution buffer (up to 400 μl in total) was added for input. The samples were nutated for 1 h at room temperature. To reverse the cross-linking, after centrifugation, supernatant was transferred to new Eppendorf tubes, and a final concentration of 200 mM NaCl was added to each sample, followed by 65 °C water bath incubation for >6 h. The next day, 8 μl of 0.5 M EDTA, 16 μl of 1 M Tris-HCl at pH 6.5, and 1.5 μl of proteinase K were added to each sample, followed by 65 °C water bath incubation for 1 h. To purify DNA, Qiagen's PCR purification kit was used (Qiagen), and real-time qPCR was carried out for data analysis. The primer sequences used are in Table S1.

Intraperitoneal glucose tolerance test

The mice were fasted for 16 h for the glucose tolerance test. The mice were injected with glucose (1 g/kg body weight) intraperitoneally (Sigma; G8270). Blood samples (one drop from tail vein) were obtained at the 0-, 30-, 60-, 90-, and 120-min time points to measure glucose levels using CONTOUR blood glucose monitoring system (Contour, Bayer).

Statistics

The data are expressed as S.D. or S.E. for each group, and comparisons were analyzed by Student's *t* test or analysis of variance.

Author contributions—T.-C. C., R. A. L., and N. E. G. data curation; T.-C. C., R. A. L., D. K., N. E. G., and M. D. F. formal analysis; T.-C. C., R. A. L., and S. L. T. validation; T.-C. C., R. A. L., S. L. T., D. K., N. E. G., N. Y., R. T. C., J. H. T., and J. Y. L. investigation; T.-C. C., R. A. L., and D. K. visualization; T.-C. C., R. A. L., and J.-C. W. writing-original draft; R. A. L., M. K. H., and J.-C. W. writing-review and editing; S. L. T., D. K., M. K. H., and J.-C. W. project administration; M. D. F., M. K. H., and J.-C. W. resources; M. K. H. and J.-C. W. supervision; J.-C. W. conceptualization; J.-C. W. funding acquisition; J.-C. W. methodology.

Acknowledgment—We thank Dr. Charlie Harris (Washington University) for comments on the manuscript.

References

1. Woods, C. P., Hazlehurst, J. M., and Tomlinson, J. W. (2015) Glucocorticoids and non-alcoholic fatty liver disease. *J. Steroid Biochem. Mol. Biol.* **154,** 94–103 CrossRef Medline
2. Wang, J. C., Gray, N. E., Kuo, T., and Harris, C. (2012) Regulation of triglyceride metabolism by glucocorticoid receptor. *Cell Biosci.* **2,** 19 CrossRef Medline
3. de Guia, R. M., and Herzig, S. (2015) How do glucocorticoids regulate lipid metabolism? *Adv. Exp. Med. Biol.* **872,** 127–144 CrossRef Medline
4. Hermanowski-Vosatka, A., Balkovec, J. M., Cheng, K., Chen, H. Y., Hernandez, M., Koo, G. C., Le Grand, C. B., Li, Z., Metzger, J. M., Mundt, S. S., Noonan, H., Nunes, C. N., Olson, S. H., Pikounis, B., Ren, N., *et al.* (2005) 11β-HSD1 inhibition ameliorates metabolic syndrome and prevents progression of atherosclerosis in mice. *J. Exp. Med.* **202,** 517–527 CrossRef Medline
5. Anil, T. M., Dandu, A., Harsha, K., Singh, J., Shree, N., Kumar, V. S., Lakshmi, M. N., Sunil, V., Harish, C., Balamurali, G. V., Naveen Kumar, B. S., Gopala, A. S., Pratibha, S., Sadasivuni, M., Anup, M. O., *et al.* (2014) A novel 11β-hydroxysteroid dehydrogenase type1 inhibitor CNX-010-49 improves hyperglycemia, lipid profile and reduces body weight in diet induced obese C57B6/J mice with a potential to provide cardio protective benefits. *BMC Pharmacol. Toxicol.* **15,** 43 CrossRefMedline
6. Li, G., Hernandez-Ono, A., Crooke, R. M., Graham, M. J., and Ginsberg, H. N. (2011) Effects of antisense-mediated inhibition of 11β-hydroxysteroid dehydrogenase type 1 on hepatic lipid metabolism. *J. Lipid Res.* **52,** 971–981 CrossRef Medline
7. Nuotio-Antar, A. M., Hachey, D. L., and Hasty, A. H. (2007) Carbenoxolone treatment attenuates symptoms of metabolic syndrome and atherogenesis in obese, hyperlipidemic mice. *Am. J. Physiol. Endocrinol. Metab.* **293,** E1517–E1528 CrossRef Medline
8. Stefan, N., Ramsauer, M., Jordan, P., Nowotny, B., Kantartzis, K., Machann, J., Hwang, J. H., Nowotny, P., Kahl, S., Harreiter, J., Hornemann, S., Sanyal, A. J., Stewart, P. M., Pfeiffer, A. F., Kautzky-Willer, A., *et al.* (2014) Inhibition of 11β-HSD1 with RO5093151 for non-alcoholic fatty liver disease: a multicentre, randomised, double-blind, placebo-controlled trial. *Lancet Diabetes Endocrinol.* **2,** 406–416 CrossRef Medline
9. Priyadarshini, E., and Anuradha, C. V. (2017) Glucocorticoid antagonism reduces insulin resistance and associated lipid abnormalities in high-fructose-Fed mice. *Can. J. Diabetes* **41,** 41–51 CrossRef Medline
10. Luz, J. G., Carson, M. W., Condon, B., Clawson, D., Pustilnik, A., Kohlman, D. T., Barr, R. J., Bean, J. S., Dill, M. J., Sindelar, D. K., Maletic, M., and Coghlan, M. J. (2015) Indole glucocorticoid receptor antagonists active in a model of dyslipidemia act via a unique association with an agonist binding site. *J. Med. Chem.* **58,** 6607–6618 CrossRef Medline
11. Dolinsky, V. W., Douglas, D. N., Lehner, R., and Vance, D. E. (2004) Regulation of the enzymes of hepatic microsomal triacylglycerol lipolysis and re-esterification by the glucocorticoid dexamethasone. *Biochem. J.* **378,** 967–974 CrossRef Medline
12. Berdanier, C. D. (1989) Role of glucocorticoids in the regulation of lipogenesis. *Faseb J.* **3,** 2179–2183 CrossRef Medline
13. Amatruda, J. M., Danahy, S. A., and Chang, C. L. (1983) The effects of glucocorticoids on insulin-stimulated lipogenesis in primary cultures of rat hepatocytes. *Biochem. J.* **212,** 135–141 CrossRef Medline
14. Nasiri, M., Nikolaou, N., Parajes, S., Krone, N. P., Valsamakis, G., Mastorakos, G., Hughes, B., Taylor, A., Bujalska, I. J., Gathercole, L. L., and Tomlinson, J. W. (2015) 5α-Reductase type 2 regulates glucocorticoid action and metabolic phenotype in human hepatocytes. *Endocrinology* **156,** 2863–2871 CrossRef Medline
15. Arnaldi, G., Scandali, V. M., Trementino, L., Cardinaletti, M., Appolloni, G., and Boscaro, M. (2010) Pathophysiology of dyslipidemia in Cushing's syndrome. *Neuroendocrinology* **92,** (Suppl. 1) 86–90 CrossRef Medline
16. Seckl, J. R., Morton, N. M., Chapman, K. E., and Walker, B. R. (2004) Glucocorticoids and 11β-hydroxysteroid dehydrogenase in adipose tissue. *Recent Prog. Horm. Res.* **59,** 359–393 CrossRef Medline
17. Koliwad, S. K., Kuo, T., Shipp, L. E., Gray, N. E., Backhed, F., So, A. Y., Farese, R. V., Jr, and Wang, J. C. (2009) Angiopoietin-like 4 (ANGPTL4, fasting-induced adipose factor) is a direct glucocorticoid receptor target and participates in glucocorticoid-regulated triglyceride metabolism. *J. Biol. Chem.* **284,** 25593–25601 CrossRef Medline
18. Gray, N. E., Lam, L. N., Yang, K., Zhou, A. Y., Koliwad, S., and Wang, J. C. (2012) Angiopoietin-like 4 (Angptl4) protein is a physiological mediator of intracellular lipolysis in murine adipocytes. *J. Biol. Chem.* **287,** 8444–8456 CrossRef Medline
19. Chen, T. C., Benjamin, D. I., Kuo, T., Lee, R. A., Li, M. L., Mar, D. J., Costello, D. E., Nomura, D. K., and Wang, J. C. (2017) The glucocorticoid-Angptl4-ceramide axis induces insulin resistance through PP2A and PKCζ. *Sci. Signal.* **10,** eaai7905 CrossRef Medline
20. Pagadala, M., Kasumov, T., McCullough, A. J., Zein, N. N., and Kirwan, J. P. (2012) Role of ceramides in nonalcoholic fatty liver disease. *Trends Endocrinol Metab.* **23,** 365–371 CrossRef Medline
21. Kasumov, T., Li, L., Li, M., Gulshan, K., Kirwan, J. P., Liu, X., Previs, S., Willard, B., Smith, J. D., and McCullough, A. (2015) Ceramide as a mediator of non-alcoholic fatty liver disease and associated atherosclerosis. *PLoS One* **10,** e0126910 CrossRef Medline
22. Kurek, K., Piotrowska, D. M., Wiesiolek-Kurek, P., Lukaszuk, B., Chabowski, A., Górski, J., and Zendzian-Piotrowska, M. (2014) Inhibition of ceramide de novo synthesis reduces liver lipid accumulation in rats with nonalcoholic fatty liver disease. *Liver Int.* **34,** 1074–1083 CrossRef Medline
23. Jeon, T. I., and Osborne, T. F. (2012) SREBPs: metabolic integrators in physiology and metabolism. *Trends Endocrinol Metab.* **23,** 65–72 CrossRef Medline
24. Wang, Y., Viscarra, J., Kim, S. J., and Sul, H. S. (2015) Transcriptional regulation of hepatic lipogenesis. *Nat. Rev. Mol. Cell Biol.* **16,** 678–689 CrossRef Medline
25. Herman, M. A., Peroni, O. D., Villoria, J., Schön, M. R., Abumrad, N. A., Blüher, M., Klein, S., and Kahn, B. B. (2012) A novel ChREBP isoform in adipose tissue regulates systemic glucose metabolism. *Nature* **484,** 333–338 CrossRef Medline
26. Baraille, F., Planchais, J., Dentin, R., Guilmeau, S., and Postic, C. (2015) Integration of ChREBP-mediated glucose sensing into whole body metabolism. *Physiology* (*Bethesda*) **30,** 428–437 CrossRef Medline
27. Miyake, Y., Kozutsumi, Y., Nakamura, S., Fujita, T., and Kawasaki, T. (1995) Serine palmitoyltransferase is the primary target of a sphingosine-like immunosuppressant, ISP-1/myriocin. *Biochem. Biophys. Res. Commun.* **211,** 396–403 CrossRef Medline
28. Sajan, M. P., Ivey, R. A., Lee, M. C., and Farese, R. V. (2015) Hepatic insulin resistance in ob/ob mice involves increases in ceramide, aPKC activity, and selective impairment of Akt-dependent FoxO1 phosphorylation. *J. Lipid Res.* **56,** 70–80 CrossRef Medline
29. Xia, J. Y., Holland, W. L., Kusminski, C. M., Sun, K., Sharma, A. X., Pearson, M. J., Sifuentes, A. J., McDonald, J. G., Gordillo, R., and Scherer, P. E. (2015) Targeted induction of ceramide degradation leads to improved

systemic metabolism and reduced hepatic steatosis. *Cell Metab.* **22,** 266–278 CrossRef Medline

30. Baranowski, M., B. A., Zabielski, P., and Górski, J. (2007) PPARα agonist induces the accumulation of ceramide in the heart of rats fed high-fat diet. *J. Physiol. Pharmacol.* **58,** 57–72 Medline
31. Aye, I. L., Gao, X., Weintraub, S. T., Jansson, T., and Powell, T. L. (2014) Adiponectin inhibits insulin function in primary trophoblasts by PPAR-mediated ceramide synthesis. *Mol. Endocrinol.* **28,** 512–524 CrossRef Medline
32. Rivier, M., Castiel, I., Safonova, I., Ailhaud, G., and Michel, S. (2000) Peroxisome proliferator-activated receptor-α enhances lipid metabolism in a skin equivalent model. *J. Invest. Dermatol.* **114,** 681–687 CrossRef Medline
33. Bernal-Mizrachi, C., Weng, S., Feng, C., Finck, B. N., Knutsen, R. H., Leone, T. C., Coleman, T., Mecham, R. P., Kelly, D. P., and Semenkovich, C. F. (2003) Dexamethasone induction of hypertension and diabetes is PPAR-α dependent in LDL receptor-null mice. *Nat. Med.* **9,** 1069–1075 CrossRef Medline
34. Ge, H., Cha, J. Y., Gopal, H., Harp, C., Yu, X., Repa, J. J., and Li, C. (2005) Differential regulation and properties of angiopoietin-like proteins 3 and 4. *J. Lipid Res.* **46,** 1484–1490 CrossRef Medline
35. Yau, M. H., Wang, Y., Lam, K. S., Zhang, J., Wu, D., and Xu, A. (2009) A highly conserved motif within the NH_2-terminal coiled-coil domain of angiopoietin-like protein 4 confers its inhibitory effects on lipoprotein lipase by disrupting the enzyme dimerization. *J. Biol. Chem.* **284,** 11942–11952 CrossRef Medline
36. McQueen, A. E., Kanamaluru, D., Yan, K., Gray, N. E., Wu, L., Li, M. L., Chang, A., Hasan, A., Stifler, D., Koliwad, S. K., and Wang, J. C. (2017) The C-terminal fibrinogen-like domain of angiopoietin-like 4 stimulates adipose tissue lipolysis and promotes energy expenditure. *J. Biol. Chem.* **292,** 16122–16134 CrossRef Medline
37. Garg, A. (1996) Insulin resistance in the pathogenesis of dyslipidemia. *Diabetes Care* **19,** 387–389 CrossRef Medline
38. Jornayvaz, F. R., Samuel, V. T., and Shulman, G. I. (2010) The role of muscle insulin resistance in the pathogenesis of atherogenic dyslipidemia and nonalcoholic fatty liver disease associated with the metabolic syndrome. *Annu. Rev. Nutr.* **30,** 273–290 CrossRef Medline
39. Robins, S. J., Lyass, A., Zachariah, J. P., Massaro, J. M., and Vasan, R. S. (2011) Insulin resistance and the relationship of a dyslipidemia to coronary heart disease: the Framingham Heart Study. *Arterioscler. Thromb. Vasc. Biol.* **31,** 1208–1214 CrossRef Medline
40. Wang, Y., Wong, R. H., Tang, T., Hudak, C. S., Yang, D., Duncan, R. E., and Sul, H. S. (2013) Phosphorylation and recruitment of BAF60c in chromatin remodeling for lipogenesis in response to insulin. *Mol. Cell* **49,** 283–297 CrossRef Medline
41. Turpin, S. M., Nicholls, H. T., Willmes, D. M., Mourier, A., Brodesser, S., Wunderlich, C. M., Mauer, J., Xu, E., Hammerschmidt, P., Brönneke, H. S., Trifunovic, A., LoSasso, G., Wunderlich, F. T., Kornfeld, J. W., Blüher, M., *et al.* (2014) Obesity-induced CerS6-dependent C16:0 ceramide production promotes weight gain and glucose intolerance. *Cell Metab.* **20,** 678–686 CrossRef Medline
42. Raichur, S., Wang, S. T., Chan, P. W., Li, Y., Ching, J., Chaurasia, B., Dogra, S., Öhman, M. K., Takeda, K., Sugii, S., Pewzner-Jung, Y., Futerman, A. H., and Summers, S. A. (2014) CerS2 haploinsufficiency inhibits β-oxidation and confers susceptibility to diet-induced steatohepatitis and insulin resistance. *Cell Metab.* **20,** 687–695 CrossRef Medline
43. Bäckhed, F., Ding, H., Wang, T., Hooper, L. V., Koh, G. Y., Nagy, A., Semenkovich, C. F., and Gordon, J. I. (2004) The gut microbiota as an environmental factor that regulates fat storage. *Proc. Natl. Acad. Sci. U.S.A.* **101,** 15718–15723 CrossRef Medline
44. Hellerstein, M. K., Christiansen, M., Kaempfer, S., Kletke, C., Wu, K., Reid, J. S., and Mulligan, K., Hellerstein, N. S., and Shackleton, C. H. (1991) Measurement of *de novo* hepatic lipogenesis in humans using stable isotopes. *J. Clin. Invest.* **87,** 1841–1852 CrossRef Medline
45. Hellerstein, M. K., and Neese, R. A. (1992) Mass isotopomer distribution analysis: a technique for measuring biosynthesis and turnover of polymers. *Am. J. Physiol.* **263,** E988–E1001 Medline
46. Kong, L., Ren, W., Li, W., Zhao, S., Mi, H., Wang, R., Zhang, Y., Wu, W., Nan, Y., and Yu, J. (2011) Activation of peroxisome proliferator activated receptor α ameliorates ethanol induced steatohepatitis in mice. *Lipids Health Dis.* **10,** 246 CrossRef Medline
47. Xie, L., Liu, C., Wang, L., Gunawardena, H. P., Yu, Y., Du, R., Taxman, D. J., Dai, P., Yan, Z., Yu, J., Holly, S. P., Parise, L. V., Wan, Y. Y., Ting, J. P., and Chen, X. (2013) Protein phosphatase 2A catalytic subunit α plays a MyD88-dependent, central role in the gene-specific regulation of endotoxin tolerance. *Cell Reports* **3,** 678–688 CrossRef Medline
48. Kuo, T., Chen, T. C., Yan, S., Foo, F., Ching, C., McQueen, A., and Wang, J. C. (2014) Repression of glucocorticoid-stimulated angiopoietin-like 4 gene transcription by insulin. *J. Lipid Res.* **55,** 919–928 CrossRef Medline
49. da Silva Xavier, G., Rutter, G. A., Diraison, F., Andreolas, C., and Leclerc, I. (2006) ChREBP binding to fatty acid synthase and L-type pyruvate kinase genes is stimulated by glucose in pancreatic β-cells. *J. Lipid Res.* **47,** 2482–2491 CrossRef Medline